

Structural characterization of electrochemically and *in vitro* biologically generated oxidation products of atorvastatin using UHPLC/MS/MS

Robert Jirásko · Tomáš Mikysek · Vitaliy Chagovets ·
Ivan Vokřál · Michal Holčápek

Received: 18 March 2013 / Revised: 21 May 2013 / Accepted: 10 June 2013 / Published online: 17 July 2013
© Springer-Verlag Berlin Heidelberg 2013

Abstract Ultrahigh-performance liquid chromatography coupled with high-mass-accuracy tandem mass spectrometry (UHPLC–MS–MS) has been used for elucidation of the structures of oxidation products of atorvastatin (AT), one of the most popular commercially available drugs. The purpose of the study was identification of AT metabolites in rat hepatocytes and comparison with electrochemically generated oxidation products. AT was incubated with rat hepatocytes for 24 h. Electrochemical oxidation of AT was performed by use of a three-electrode off-line system with a glassy carbon working electrode. Three supporting electrolytes (0.1 mol L⁻¹ H₂SO₄, 0.1 mol L⁻¹ HCl, and 0.1 mol L⁻¹ NaCl) were tested, and dependence on pH was also investigated. AT undergoes oxidation by a single irreversible process at approximately +1.0 V vs. Ag/AgCl electrode. The results obtained revealed a simple and relatively fast way of determining the type of oxidation and its position, on the basis of characteristic neutral losses (NLs) and fragment ions. Unfortunately, different products were obtained by electrochemical oxidation and biotransformation of AT. High-mass-accuracy measurement combined with different UHPLC–MS–MS scans, for example reconstructed ion-current chromatograms, constant neutral loss chromatograms, or exact mass

filtering, enable rapid identification of drug-related compounds. β -Oxidation, aromatic hydroxylation of the phenylaminocarbonyl group, sulfation, AT lactone and glycol formation were observed in rat biotransformation samples. In contrast, a variety of oxidation reactions on the conjugated skeleton of isopropyl substituent of AT were identified as products of electrolysis.

Keywords Atorvastatin · Electrochemical generation · Ultrahigh-performance liquid chromatography–tandem mass spectrometry · Biotransformation · Drug metabolism

Introduction

Atorvastatin (Fig. 1), an inhibitor of 3-hydroxy-3-methylglutaryl-CoA reductase, belongs to the group of statins used in hyperlipidemia therapy [1]. AT has been, and still is, one of the most popular commercially available drugs (the best-selling drug in the history). Most published articles are related to its determination in biological samples [2–5], characterization of its metabolism [6–13], and description of its oxidative degradation products [14, 15].

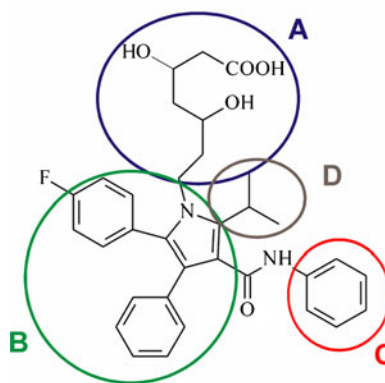
Study of drug metabolism is a crucial task in pharmaceutical research. *In-vitro* and *in-vivo* experiments based on enzymatically catalyzed reactions are usually performed for simulation of oxidative or reductive metabolism [16–18], but on-line or off-line electrochemical oxidation or reduction can also be helpful for prediction of possible metabolites without the use of laboratory animals [19–28]. Glassy carbon or precious metal (Pt, Au) electrodes are used as working electrodes in electrochemical generation of oxidation products [27, 29] and the mercury-pool electrode can be used for generation of reduction products. Electrochemical oxidation has been

ABC Highlights: authored by *Rising Stars and Top Experts*

R. Jirásko (✉) · T. Mikysek · V. Chagovets · M. Holčápek
Department of Analytical Chemistry, Faculty of Chemical
Technology, University of Pardubice, Studentská 573, 53210
Pardubice, Czech Republic
e-mail: Robert.Jirasko@upce.cz

I. Vokřál
Department of Pharmacology and Toxicology, Faculty of
Pharmacy in Hradec Králové, Charles University in Prague,
Heyrovského 1203, 50005 Hradec Králové, Czech Republic

Fig. 1 Chemical structure of atorvastatin (AT) composed of four main parts, denoted as A, B, C, and D, including a list of identified oxidation reactions for both electrochemical and *in-vitro* experiments



Biotransformation products:

- 1) aryl hydroxylation (part C)
- 2) β -oxidation (part A)
- 3) lactone and glycol formation (part A)
- 4) sulfatation (part C)
- 5) combination of mechanisms

Electrochemically generated products:

- 1) lactone formation (part A)
- 2) methyl ester formation (part A)
- 3) oxidation (+O) of conjugated skeleton (part B)
- 4) propyl oxidation (-H₂ or +O) - part D
- 5) combination of mechanisms

successfully used for simulation of the phase I metabolism of several pharmaceutical compounds, e.g., tetrazepam [19], paracetamol (acetaminophen) [30–32], and clozapine [30, 33, 34]. Formation of phase II metabolites can also be achieved in the presence of a specific enzymatic or non-enzymatic catalyst, for example, enzymatically catalyzed formation of the glutathione conjugate of toremifene, a selective estrogen receptor modulator, by use of glutathione-S-transferase, was performed in an on-line electrochemical system [26]. In general, electrochemical prediction of biological oxidative processes can be used for all compounds predisposed to oxidative or reductive reactions, mainly for environmentally and pharmaceutically important compounds. In addition, electrochemical generation followed by purification (preparative HPLC or thin-layer chromatography) can be used for electro-synthesis of expensive or unavailable drug metabolite standards. The efficiency of synthesis depends on the size and character of the working electrode used for product generation, and mixing must be sufficient to avoid electrode blocking by products. Electrochemistry can also provide information about labile sites in a molecule sensitive to oxidation and reduction [26].

An important aspect of electrochemical metabolite generation is reliable analytical characterization of generated compounds to verify their exact structures and for subsequent comparison with human or animal biotransformation products [19, 29, 35, 36]. Moreover, generated products can be affected by the chemicals used during sample preparation, so comparison with blank samples is required to find possible degradation products. HPLC–MS–MS is usually the method of choice for metabolic studies because of its high sensitivity and the possibility of obtaining structural information even for trace metabolites in highly complex matrices [18, 37]. Several strategies, for example use of selected tandem mass spectrometric scans, ion mobility mass spectrometry, on-line H/D exchange HPLC–MS–MS, accurate mass measurements, radiolabeling of parent drugs, chemical derivatization to determine the position of metabolic reaction or to improve ionization efficiency, and software dedicated to metabolite prediction or detection, can be used for this purpose [38–45].

In this study UHPLC–MS–MS was used for elucidation of the structures of the oxidation products of AT in electrochemical and *in-vitro* experiments, on the basis of a combination of retention behavior and high-mass-accuracy tandem mass spectrometry.

Materials and methods

Chemicals and reagents

Atorvastatin (3*R*,5*R*)-7-[2-(4-fluorophenyl)-3-phenyl-4-(phenylcarbamoyl)-5-propan-2-ylpyrrol-1-yl]-3,5-dihydroxyheptanoic acid calcium trihydrate was purchased from the European Directorate for the Quality of Medicines and HealthCare Council of Europe (Strasbourg, France). Acetonitrile, methanol, formic acid, acetic acid, ammonium acetate, sodium formate, Ham's F12, William's E, collagenase type IV, dimethyl sulfoxide, and fetal bovine calf serum were purchased from Sigma–Aldrich (St Louis, MO, USA). Deionized water was prepared with a Demiwa 5-roi purification system (Watek, Ledec nad Sázavou, Czech Republic). The supporting electrolytes (HCl, NaCl, H₂SO₄) were prepared at a concentration of 0.1 mol L⁻¹. A series of Britton–Robinson buffers for study of the effect of pH in the range 2–12 was prepared in accordance with the recommended procedure in a common laboratory handbook.

Isolation of hepatocytes and incubation with AT in the *in-vitro* experiment

Rats were cared for and used in accordance with the *Guide for the care and use of laboratory animals* (Protection of Animals from Cruelty Act. No. 246/92, Czech Republic). Hepatocytes were obtained from the liver of a male rat by the two-step collagenase method. Three million viable (72 %) cells in 3 mL culture medium ISOM (1:1 mixture of Ham's F12 and William's E) were placed in 60-mm plastic Petri dishes pre-coated with collagen. Fetal bovine calf serum was

added to the culture medium (5 %) to promote cell attachment during the first four hours. During this period, cultures were maintained without the substrate at 37 °C in a humid atmosphere of air and 5 % CO₂. After attachment of the hepatocytes, the medium was replaced with fresh serum-free medium containing AT (10 μmol L⁻¹). AT was pre-dissolved in dimethyl sulfoxide. The final concentration of dimethyl sulfoxide in the medium did not exceed 0.1 %. After 24 h at 37 °C in a humid atmosphere of air and 5 % CO₂, hepatocytes were scraped from the plate and homogenized.

Electrochemical experiments

A standard stock solution of AT ($c = 1 \text{ mg mL}^{-1}$) was prepared by dissolving the compound in methanol. Cyclic voltammetry (CV) and electrolytic experiments were performed by use of the PGSTAT 128 N electrochemical analyzer (Autolab, Metrohm Autolab, Utrecht, The Netherlands) operated by use of NOVA 1.8 software. All electrochemical experiments were performed with a three-electrode system comprising Ag/AgCl/3 mol L⁻¹ KCl separated by a bridge filled with the supporting electrolyte as the reference electrode, Pt sheet (ca. 10 mm × 5 mm) as counter electrode, and a working electrode selected on the basis of the experiment performed—glassy carbon (2 mm diameter) for CV experiments and a large-area (geometric area 2.2 cm²) pyrolytic graphite electrode for electrolysis. Preparative electrolysis and coulometric measurements were performed in a two-compartment H-type cell (Fig. 2) containing 10 mL electrolyzed solution. In principal, the H-type cell can be used for either oxidation or reduction, depending on the type of working electrode. 0.1 mol L⁻¹ H₂SO₄, 0.1 mol L⁻¹ HCl, or 0.1 mol L⁻¹ NaCl were used as solutions for electrolysis; the concentration of the compound electrolyzed was approximately 0.1 mg mL⁻¹ and the duration of electrolysis between 1 and 2 h, depending on the potential applied. Potentiostatic coulometry was used for evaluation of

the number of electrons involved in the electrode reactions; Autolab software was used for integration of current flow.

Solid-phase extraction (SPE)

Samples were centrifuged at 3000g for 5 min. The supernatant was extracted by use of SPE. The sample was loaded on to a Phenomenex Strata X (1 mL, 30 mg, 33 μm; Phenomenex, Torrance, California, USA) extraction cartridge previously preconditioned by washing with 1 mL acetonitrile and 1 mL purified water. In the next step, the cartridge was washed with 2 mL 15 % (v/v) acetonitrile–water. Compounds of interest were eluted with 1 mL acetonitrile. Samples were evaporated to dryness under a nitrogen stream. Dry samples were quantitatively dissolved in 300 μL 50:50 (v/v) acetonitrile–water and injected for UHPLC–MS analysis.

UHPLC–MS–MS conditions

UHPLC–MS–MS chromatograms of samples were acquired by use of electrospray ionization (ESI) on a hybrid quadrupole time-of-flight mass analyzer (micrOTOF-Q; Bruker Daltonics, Germany). UHPLC was performed on an Agilent 1290 Infinity liquid chromatograph (Agilent Technologies, Waldbronn, Germany) equipped with a Zorbax Eclipse C₁₈ column (150 mm × 2.1 mm, 1.8 μm; Agilent). The analysis temperature was 25 °C, the flow rate 0.4 mL min⁻¹, and the injection volume 0.1 μL. The mobile phase was a gradient prepared from 0.5 mmol L⁻¹ ammonium acetate adjusted to pH 4.0 (component A) and acetonitrile (component B). The linear gradient was: 0 min, 50 % B; 6 min, 56 % B; 9 min, 95 % B; and, finally, washing and reconditioning of the column. The QqTOF mass spectrometer was used with the settings: capillary voltage 4.5 kV, drying temperature 220 °C, and flow rate and pressure of nitrogen 8 L min⁻¹ and 1.3 bar, respectively. External calibration was performed with sodium formate clusters before individual measurements. ESI mass spectra were recorded in the range m/z 50–1000 in both positive-ion and negative-ion modes. An isolation width, $\Delta m/z$, of 4 and a collision energy of 20–30 eV, with argon as collision gas, were used for MS–MS experiments.



Fig. 2 Schematic diagram of electrochemical H-type cell: 1, working electrode (glassy carbon or pyrolytic graphite electrode); 2, auxiliary electrode (platinum sheet); 3, reference electrode (Ag/AgCl/3 mol L⁻¹ KCl); 4, inlet of argon for bubbling; 5, glass frit

Results and discussion

AT and its electrochemical oxidation and biotransformation products (Fig. 1) were analyzed by use of UHPLC–MS–MS with ESI. The mobile phase used resulted in high ionization efficiency and satisfactory sensitivity even for metabolites of low abundance. The structures of the oxidation products were determined on the basis of their chromatographic behavior; chromatographic peaks were distributed over the whole chromatogram (Tables 1 and 2). Use of different UHPLC–MS–MS

scans, for example reconstructed ion current chromatograms, constant neutral loss chromatograms, and mass defect filtering, enabled detection and unambiguous identification of compounds originating from the drug. To avoid false positive results and distinguish metabolites from possible degradation products, comparison with blank samples was performed for both electrochemically and biologically generated compounds. Determination of the elemental composition of individual oxidation products was based on accurate masses, typically better than 3 ppm mass accuracy even with the external calibration. The character of ions observed in mass spectra depends on many factors, for example type of ionization, polarity, applied potentials, solvents used, and the structures of the compounds studied. Formation of protonated molecules in positive-ion full-scan mass spectra or deprotonated molecules in negative-ion full-scan mass spectra were the main mechanisms of ion formation. These typical ions were accompanied by adduct ions, for example $[M + Na]^+$ and $[M + K]^+$ in positive-ion or $[M + Cl]^-$ in negative-ion full-scan mass spectra for most observed metabolites. Although ammonium acetate was used in the mobile phase, no $[M + NH_4]^+$ or $[M + CH_3COO]^-$ ions were found in full-scan mass spectra except for E8a, b. In the text below, the annotation “E” refers to electrochemically generated products (Table 2) whereas “M” is used for biotransformation metabolites (Table 1). The ions observed provided clear information about molecular weights and elemental compositions of detected

compounds. Interpretation of tandem mass spectra was important in characterization of the structures of these oxidation products, because of the presence of many metabolites with the same elemental composition (Tables 1 and 2). Characteristic fragment ions and typical neutral losses (NLs) for both polarity modes aided elucidation of the structures of unknown compounds. The structure of AT can be divided into four basic parts (Fig. 1; annotated as A, B, C, and D). Each part of molecule can be associated with characteristic NLs and fragment ions. Most important NLs and fragment ions, which provided information about the structure of AT, are shown in Fig. 3.

UHPLC–MS of *in-vitro*-generated metabolites

In total, nine phase I metabolites and one phase II metabolite (AT sulfate) were identified in the rat biotransformation samples studied (Table 1 and Fig. 4a). In general, these AT metabolic products can be associated with three metabolic reactions: aryl-oxidation, β -oxidation, and lactone formation. In rat biotransformation of AT, β -oxidation was the prevailing metabolic pathway. The corresponding shifts in retention behavior in reversed-phase chromatography were in accordance with the structures of the metabolites identified. Reduced retention was recorded for hydroxylated and sulfate metabolites (M1 and M4) whereas increased retention compared with the parent AT was observed for β -oxidation

Table 1 List of main peaks from *in-vitro* biotransformation of atorvastatin, detected by UHPLC–MS–MS, with their numbering, retention times, experimental m/z values of $[M + H]^+$ and $[M - H]^-$ ions in ESI

No.	t_R (min)	Experimental m/z values of important ions (mass accuracy in ppm)		MW	Elemental composition	Description of oxidation reaction (oxidized part of molecule)	Important product ions of $[M + H]^+$, m/z	Important product ions of $[M - H]^-$, m/z
		$[M + H]^+$	$[M - H]^-$					
M1a	1.55	575.2567 (2.6)	573.2392 (−2.4)	574	$C_{33}H_{35}FN_2O_6$	AT + O (part C)	466; 440; 380; 292; 250	469; 413; 278
M1b	3.03	575.2555 (0.5)	573.2401 (−0.9)				466; 440; 380; 292; 250	413; 278; 134
M2	8.22	499.2402 (2.0)	497.2254 (1.6)	498	$C_{31}H_{31}FN_2O_3$	β -oxidized AT	457; 406; 399; 380	397; 278
M3a	3.58	515.2356 (2.9)	513.2186 (−1.8)	514	$C_{31}H_{31}FN_2O_4$	β -oxidized AT + O	406; 380; 338	413; 278
M3b	7.71	515.2335 (−1.2)	513.2183 (−2.3)			(part C)	406; 380; 338	413; 278; 134
M4	1.75	n.d. ^a	593.1750 (−2.2)	594	$C_{31}H_{31}FN_2O_7S$	β -oxidized AT + O + SO_3 (part C)	–	513; 413; 278
M5	4.64	515.2340 (−0.2)	513.2185 (−1.9)	514	$C_{31}H_{31}FN_2O_4$	β -oxidized AT + O (part A)	422; 396; 354	453; 397; 278
M6	6.59	541.2480 (−3.1)	n.d. ^a	540	$C_{33}H_{33}FN_2O_4$	AT lactone	422; 292 (low intensity)	–
M7	5.79	543.2661 (1.3)	541.2491 (−3.1)	542	$C_{33}H_{35}FN_2O_4$	AT glycol	450; 424; 364; 292; 250	523; 397; 278
M8	4.89	n.d. ^a	557.2447 (−1.8)	558	$C_{33}H_{35}FN_2O_5$	AT glycol + O (part C)	–	541; 278; 134
AT	3.60	559.2602 (0.7)	557.2455 (−0.4)	558	$C_{33}H_{35}FN_2O_5$	Initial drug	466; 440; 292; 250	453; 397; 278

^a Not detected

+ O hydroxylation, + SO_3 sulfation

Table 2 List of main peaks from electrochemical oxidation of AT in 0.1 mol L⁻¹ HCl, detected by UHPLC-MS-MS, with their numbering, retention times, experimental *m/z* values of [M + H]⁺ and [M - H]⁻ ions in ESI full-scan mass spectra, mass accuracies, molecular weights (MW), elemental composition, description of metabolites present, and MS-MS product ions

No.	<i>t_R</i> (min)	Experimental <i>m/z</i> values of important ions (mass accuracy in ppm)		MW	Elemental composition	Description of oxidation reaction (changed part of molecule)	Important product ions of [M + H] ⁺ , <i>m/z</i>	Important product ions of [M - H] ⁻ , <i>m/z</i>
		[M + H] ⁺	[M - H] ⁻					
E1a	1.30	575.2556 (0.7)	573.2413 (1.2)	574	C ₃₃ H ₃₅ FN ₂ O ₆	AT + O (part B)	557; 456; 438 413; 308	454; 413; 294
E1b	2.92	575.2558 (1.0)	573.2394 (-2.1)				557; 308; 250	469; 413; 294
E1c	3.60	575.2562 (1.7)	573.2416 (1.7)				557; 515; 438; 308; 294	454; 436; 392; 350; 294
E2	1.94	n.d. ^a	573.2400 (-1.0)	574	C ₃₃ H ₃₅ FN ₂ O ₆	AT + O (part D)	–	413; 355
E3a	1.91	549.2021 (-2.0)	547.1891 (0.9)	548	C ₃₀ H ₂₉ FN ₂ O ₇	AT - propene + 2*O (part B)	–	428; 268; 225
E3b	2.05	n.d. ^a	547.1870 (-2.9)				–	428; 410; 268; 225
E4a	3.10	531.1924 (-0.4)	529.1771 (-1.7)	530	C ₃₀ H ₂₇ FN ₂ O ₆	AT lactone - propene + 2*O (part B)	383; 234	410; 268; 225
E4b	3.30	531.1934 (1.5)	529.1777 (-0.6)				383; 355; 234	410; 350; 268; 225
E4c	3.38	531.1932 (1.1)	529.1776 (-0.7)				438; 383; 234	469; 410; 350; 268
E5a	3.49	557.2453 (1.3)	555.2303 (0.4)	556	C ₃₃ H ₃₃ FN ₂ O ₅	AT - H ₂ (part B or D)	464; 438; 290; 250	451; 395; 276
E5b	4.01	557.2470 (2.3)	555.2307 (1.1)				464; 438; 420; 290; 250	395; 355; 276; 236
E6a	5.15	557.2467 (1.8)	555.2305 (0.7)	556	C ₃₃ H ₃₃ FN ₂ O ₅	AT lactone + O (part B or D)	464; 427; 350; 306; 294	413; 294
E6b	5.85	557.2466 (1.6)	555.2316 (2.7)				438; 308; 294	436; 294
E6c	6.08	557.2468 (2.0)	555.2314 (1.3)				464; 438; 308; 294	436; 294
E6d	6.26	557.2463 (1.1)	555.2304 (0.5)				515; 438; 308; 294	436; 294
E7a	6.43	539.2347 (1.1)	537.2186 (-1.7)	538	C ₃₃ H ₃₁ FN ₂ O ₄	AT lactone - H ₂	446; 420; 402; 318; 290	395; 276
E7b	8.57	539.2341 (0.1)	n.d. ^a				446; 420; 402; 318; 290	–
E8a	7.12	571.2598 (-0.9)	n.d. ^a	570	C ₃₄ H ₃₅ FN ₂ O ₅	AT methyl ester - H ₂	478; 452; 290; 250	–
E8b	7.98	571.2609 (1.1)	569.2456 (-1.8)				478; 452; 318; 290; 250	395; 355; 276; 236
E9	7.33	589.2712 (0.7)	n.d. ^a	588	C ₃₄ H ₃₇ FN ₂ O ₆	AT methyl ester + O	452; 308; 296	–
AT	3.60	559.2611 (1.4)	557.2464 (1.3)	558	C ₃₃ H ₃₅ FN ₂ O ₅	AT (only in blank)	466; 440; 292; 250	453; 397; 278
ATL	6.59	541.2502 (0.9)	539.2362 (1.9)	540	C ₃₃ H ₃₃ FN ₂ O ₄	AT lactone (only in blank)	448; 422; 292; 250	397; 278
ATM	7.33	573.2746 (-2.3)	571.2615 (0.2)	572	C ₃₄ H ₃₇ FN ₂ O ₅	AT methyl ester (only in blank)	480; 454; 292; 250	–

^a Not detected+ O hydroxylation or epoxidation, - H₂ dehydrogenation

products (M2, M3, and M5), AT lactone and glycol formation (M6, M7 and M8). Aryl hydroxylation of phenylaminocarbonyl, part C, the most typical metabolic reaction in humans, was observed for AT itself (M1a, b), and this mechanism was subsequently used to explain the β-oxidized metabolite, too (M3a, b). Two metabolites corresponding to aromatic hydroxylation on AT part C were detected, in accordance with the literature, in which ortho and para-hydroxylated AT metabolites have been described [11]. The elemental composition of metabolite M5 is identical with that of M3a, b, but the different fragmentation pattern revealed oxidation on AT part A (discussed in the section “[Tandem mass spectrometry for](#)

[structure elucidation](#)”). In addition to increased retention, smaller mass defects were observed for β-oxidized metabolites compared with AT, in accordance with the elemental composition change. The highest shift in the mass defect to lower values occurred for sulfate metabolite M4, because the atomic mass of sulfur (31.9721) is 0.0279 lower than the nominal mass [18]. The atorvastatin lactone (ATL) M6 was observed only in positive-ion mode, because of its low concentration, but subsequent hydrogenation to AT glycol was also recorded (M7). The aromatic hydroxylation of AT glycol (M8) was also detected in rat biotransformation. Most of the metabolic pathways observed, for example the aromatic

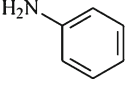
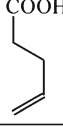
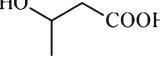
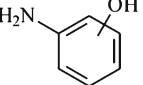
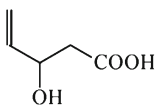
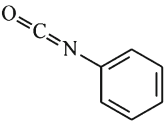
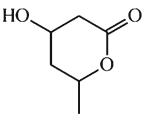
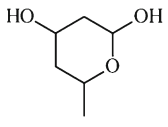
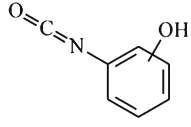
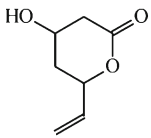
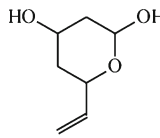
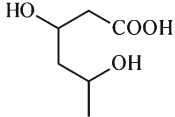
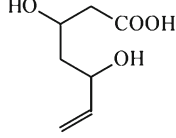
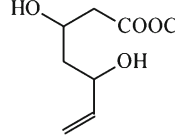
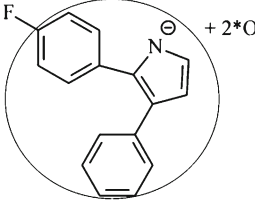
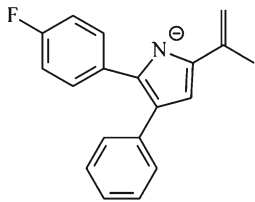
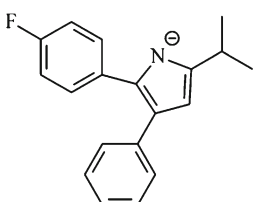
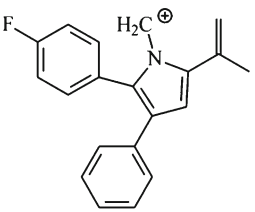
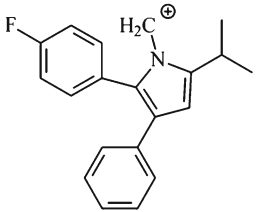
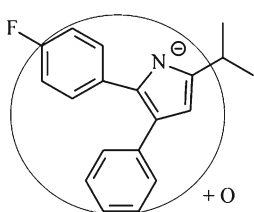
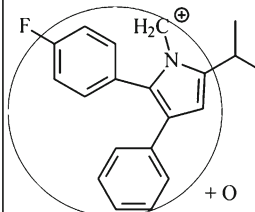
$\Delta m/z$ 42.047 C_3H_6 (unchanged part D)	$\Delta m/z$ 93.0578 C_6H_7N (unchanged part C)	$\Delta m/z$ 100.0524 $C_5H_6O_2$ (β -oxidation, part A)	$\Delta m/z$ 104.0468 $C_4H_8O_3$ (unchanged part A)	$\Delta m/z$ 109.0528 C_6H_7NO (hydroxylation, part C)
$\Delta m/z$ 58.0419 C_3H_6O (+O, part D)				
$\Delta m/z$ 116.0473 $C_5H_8O_3$ (β -oxidation and hydroxylation, part A)	$\Delta m/z$ 119.0371 C_7H_5NO (unchanged part A)	$\Delta m/z$ 130.063 $C_6H_{10}O_3$ (AT lactone, part A)	$\Delta m/z$ 132.0786 $C_6H_{12}O_3$ (AT glycol, part A)	$\Delta m/z$ 135.0320 $C_7H_5NO_2$ (hydroxylation, part C)
				
$\Delta m/z$ 142.063 $C_7H_{10}O_3$ (AT lactone, part A)	$\Delta m/z$ 144.0786 $C_7H_{12}O_3$ (AT glycol, part A)	$\Delta m/z$ 148.0736 $C_6H_{12}O_4$ (unchanged part A)	$\Delta m/z$ 160.0736 $C_7H_{12}O_4$ (unchanged part A)	$\Delta m/z$ 174.0892 $C_8H_{14}O_4$ (CH_3 ester, part A)
				
m/z 268.0779 $[C_{16}H_{11}FNO_2]^+$ (+2 \cdot O, part B)		m/z 276.1194 $[C_{19}H_{15}FN]^+$ (-H $_2$, part Bor D)		m/z 278.1350 $[C_{19}H_{17}FN]^+$ (unchanged part B)
				
m/z 290.1340 $[C_{20}H_{17}FN]^+$ (-H $_2$, part Bor D)	m/z 292.1340 $[C_{20}H_{19}FN]^+$ (unchanged part B)	m/z 294.1299 $[C_{19}H_{17}FNO]^+$ (+O, part B)	m/z 308.1445 $[C_{20}H_{19}FNO]^+$ (+O, part B)	
				

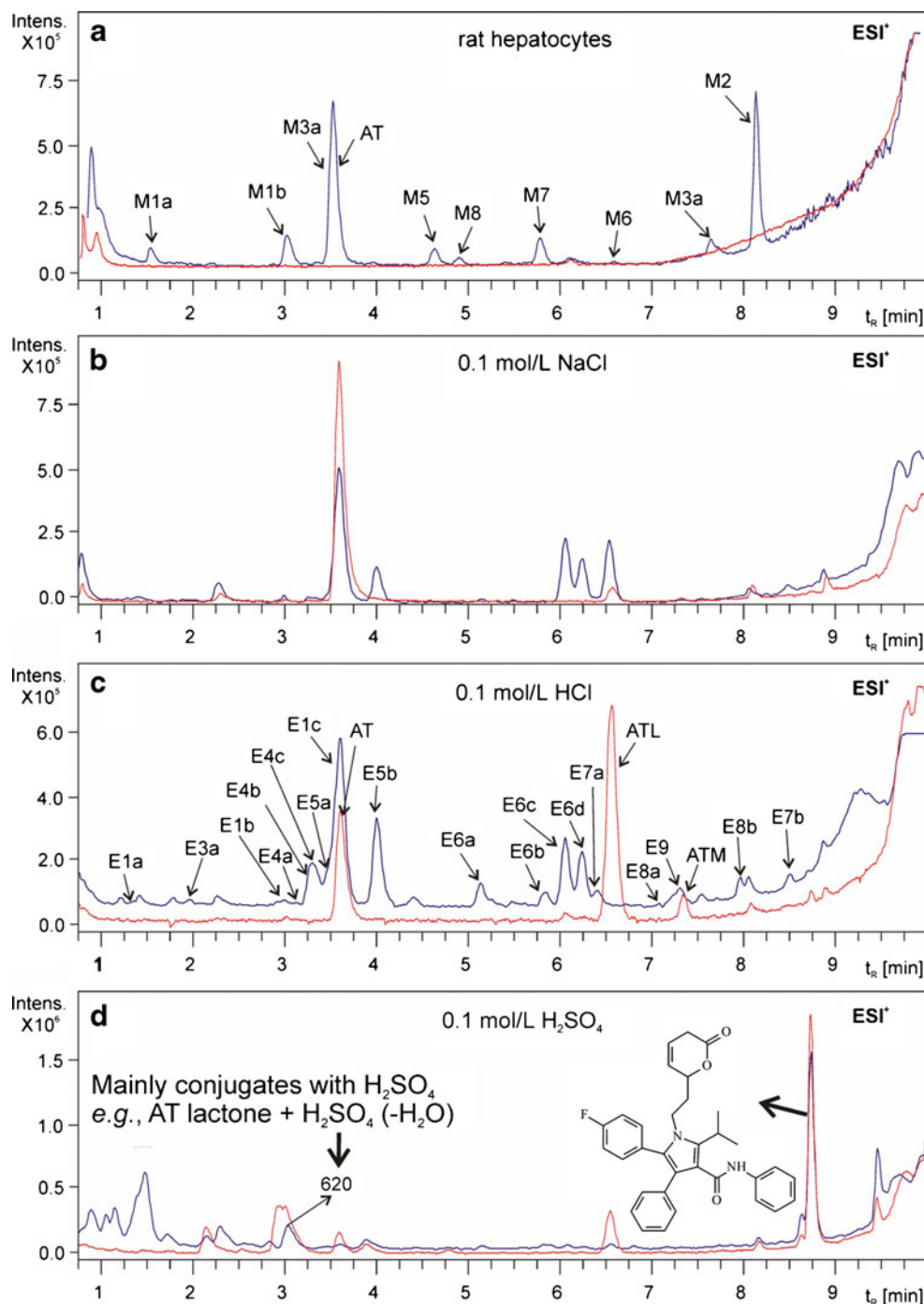
Fig. 3 Most important neutral losses and fragment ions related to the type and position of AT oxidation (the specific parts of AT are shown in Fig. 1)

hydroxylation [11, 46], β -oxidation [10], or lactone formation [9] of AT, have previously been reported, but some AT metabolites (AT glycol M7, hydroxylated AT glycol M8, and the sulfate of β -oxidized AT M4) are, to the best of our knowledge, reported here for the first time. A complete schematic diagram of rat *in-vitro* biotransformation on the basis of our experiments is shown in Fig. 5.

Description of electrochemical experiments

In our study, results from CV, coulometric, and preparative electrolysis experiments were used to obtain complete information about the electrochemical oxidative behavior of AT. Three solutions, 0.1 mol L⁻¹ H₂SO₄, 0.1 mol L⁻¹ HCl, and 0.1 mol L⁻¹ NaCl, were tested as supporting electrolytes. AT

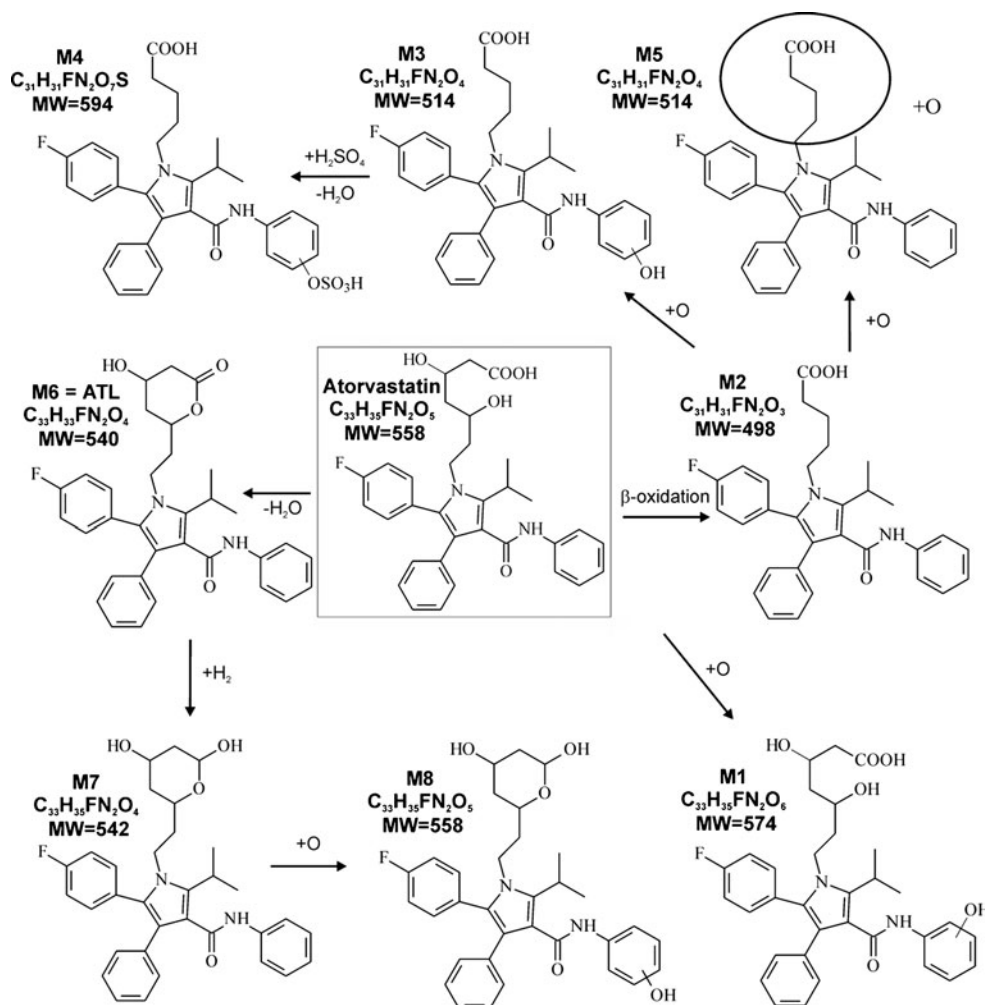
Fig. 4 TICs of AT biotransformation and electrochemical samples (blue colored): rat hepatocytes (a); electrochemical generation in 0.1 mol L⁻¹ NaCl (b); 0.1 mol L⁻¹ HCl (c), 0.1 mol L⁻¹ H₂SO₄ (d). Red colored TICs are specific chemical blanks for electrochemical samples and biological blank for rat hepatocytes (more information about the oxidation products is given in Tables 1 and 2)



undergoes the oxidation by a single irreversible process at approximately +1.0 V vs. Ag/AgCl (Fig. 6). The current decreased with each additional scan at scan rate of 50 mV s⁻¹, because of limited transport of the compound toward the electrode surface. This hypothesis was confirmed at low scan rates, for which the current does not decrease. The peak potential was shifted linearly with increasing pH to less positive values (Fig. 7a). Most of the parent AT molecules formed ATL at pH < 6 resulting in its electrochemical

activity. However, the current started to decrease at pH > 5 (Fig. 7b) and dropped to zero at higher pH, because the lactonization reaction was not fast enough and ATL and its products underwent hydrolysis. Coulometric experiments revealed that AT is oxidized by two electrons per molecule. To prove unambiguously this oxidation scheme, i.e., the formation of an intermediate and the subsequent product, controlled-potential electrolysis was performed repeatedly on the oxidation peak using acidic and neutral buffered

Fig. 5 Schematic diagram of *in vitro*-biotransformation of AT in rats



media. Unfortunately, the amounts and number of products did not enable their isolation and unambiguous identification by NMR, as was observed in another study [47].

UHPLC–MS of electrochemically treated samples

AT and its oxidation products formed during preparative electrolysis were analyzed by use of UHPLC–MS–MS with identical conditions as for rat-biotransformed samples. In contrast with the *in-vitro* study, electrochemical experiments produced compounds formed by different oxidation reactions. Figures 4b, c, and d depict the TICs of AT oxidation products generated in the media tested. Compounds corresponding to potential degradation products formed spontaneously in the solution were excluded on the basis of the comparison of chromatograms of electrochemically treated samples with the blank. The type of oxidative product was mainly affected by the supporting electrolyte. Formation of ATL is promoted in the acidic solution, as known from the literature [15]. This degradation product was observed even in the blank for all the electrolyzed solutions tested. The compound corresponding to

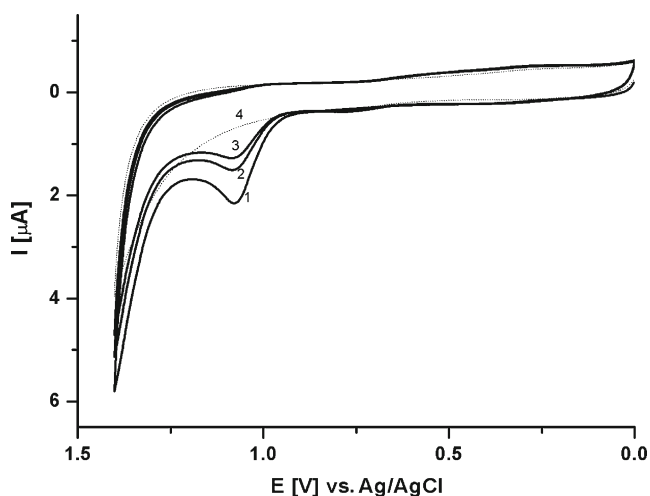


Fig. 6 Representative cyclic voltammetric curves for oxidation of AT at a glassy carbon electrode in Britton–Robinson buffer at pH 1.71. The concentration of AT was 0.05 mg mL^{-1} , the scan rate 50 mV s^{-1} , and the step potential 2.5 mV. 1, first scan; 2, second scan; 3, third scan; 4, baseline

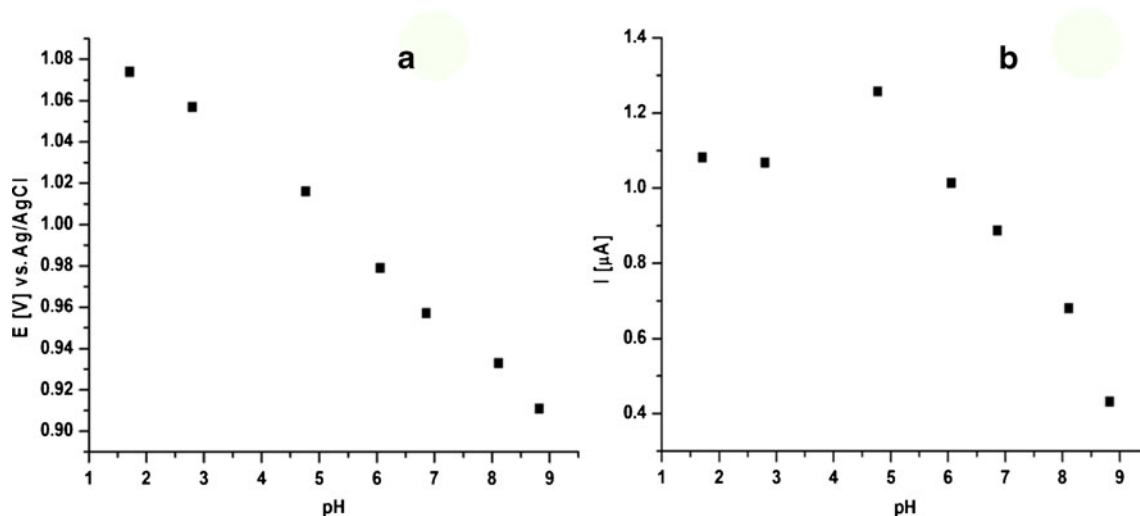


Fig. 7 Effect of pH on peak potentials (a) and currents (b) for oxidation of AT in a series of Britton–Robinson buffers. The concentration of AT was 0.1 mg mL^{-1} , the scan rate 50 mV s^{-1} , and the step potential 2.5 mV

the methyl ester of AT (ATM) was also identified in blank samples. Its formation can be explained on the basis of that methanol was used during sample preparation (“Materials and methods” section). Similar oxidation processes resulted in electrochemical oxidation of AT in $0.1 \text{ mol L}^{-1} \text{ NaCl}$ and $0.1 \text{ mol L}^{-1} \text{ HCl}$, but higher oxidation efficiency was observed at lower pH, when a higher concentration of ATL was present (Fig. 4b, c; pH-dependence curves in Fig. 7). Because of the strong dehydration effect, the most complex situation was observed for $0.1 \text{ mol L}^{-1} \text{ H}_2\text{SO}_4$ as electrolyte (Fig. 4d), in which subsequent water loss from ATL was detected. Moreover, the sulfuric acid subsequently reacted with all the compounds present to form $\text{AT} + \text{SO}_3$, $\text{ATL} + \text{SO}_3$, and $(\text{ATL} - \text{H}_2\text{O}) + \text{SO}_3$ adducts. Hence, oxidation of specific degradation products was recorded in addition to AT oxidation. Retention of the sulfuric acid adducts was shifted because of their polarity and they were eluted within 3 min.

Results obtained by use of $0.1 \text{ mol L}^{-1} \text{ HCl}$ as electrolyte are used here for detailed description of identification procedures (Table 2). Structural modifications occurred on AT parts B and D, in contrast with biotransformation, in which oxidation was observed on parts A and C (Fig. 1, Tables 1 and 2). Differences between the elemental composition of oxidation products and AT correspond to $-\text{H}_2$ (E5 and E6), $+\text{O}$ (E1 and E2), $-\text{H}_2\text{O} - \text{H}_2$ (E7), $-\text{C}_3\text{H}_6 + 2\text{O}$ (E3), $-\text{C}_3\text{H}_6 + 2\text{O} - \text{H}_2\text{O}$ (E4), $+\text{CH}_2 - \text{H}_2$ (E8), $+\text{CH}_2 + \text{O}$ (E9). All three initial compounds, AT, ATL, and ATM, must be regarded as precursors of oxidation reactions, because all were exposed to electrolysis. Information about dehydrogenation (either double-bond formation or cyclization) and addition of oxygen atoms to the molecule (hydroxylation or epoxidation) can be deduced for AT, ATL, and ATM from above mentioned differences in elemental composition. Moreover, dealkylation followed by the addition of two oxygen atoms was found for AT and ATL (oxidation products E3 and E4). On the basis of

interpretation of full-scan and tandem mass spectra, electrochemically generated oxidation products formed in $0.1 \text{ mol L}^{-1} \text{ HCl}$ medium can be divided into nine groups (Table 2) with regard to initial compound and type of oxidation.

Tandem mass spectrometry for structure elucidation

Structures and exact elemental composition of NLs and key fragment ions discussed below are shown in Fig. 3. Aromatic hydroxylation on AT part C is confirmed by NLs $\Delta m/z$ 109 and 135 (Table 1 and Fig. 8d), which are 16 mass units higher (M1a, M1b, M3a, M3b, M4, and M8) than for NLs $\Delta m/z$ 93 and 119 observed in tandem mass spectra of the parent AT and other compounds without AT part C substitution. On the other hand, information about unchanged AT part A can be obtained on the basis of observed NLs $\Delta m/z$ 160 or $\Delta m/z$ 104 in negative-ion tandem mass spectra (Tables 1, 2 and Fig. 8a) or $\Delta m/z$ 148 in positive-ion tandem mass spectra (Tables 1 and 2). Structural changes on AT part A, for example formation of AT lactone, glycol, methyl ester, or β -oxidation, were reflected in modification of the corresponding NLs. In accordance with the elemental composition change, decreases of NLs from $\Delta m/z$ 160 to $\Delta m/z$ 142 in negative-ion mode and from $\Delta m/z$ 148 to $\Delta m/z$ 130 in positive-ion mode were recorded for ATL products, whereas increased NL values were observed for ATM compounds (Figs. 3 and 8j). Identical NL $\Delta m/z$ 100 in both polarity modes was present in MS–MS of β -oxidized metabolites except for M5, for which NL $\Delta m/z$ 116 confirmed subsequent hydroxylation on AT part A (Fig. 8c). For sulfate metabolite M4, the characteristic NL $\Delta m/z$ 80 (SO_3) was followed by NLs $\Delta m/z$ 100 and $\Delta m/z$ 135, which furnished information about β -oxidation on AT part A and aromatic hydroxylation on part C (Fig. 8b). NLs

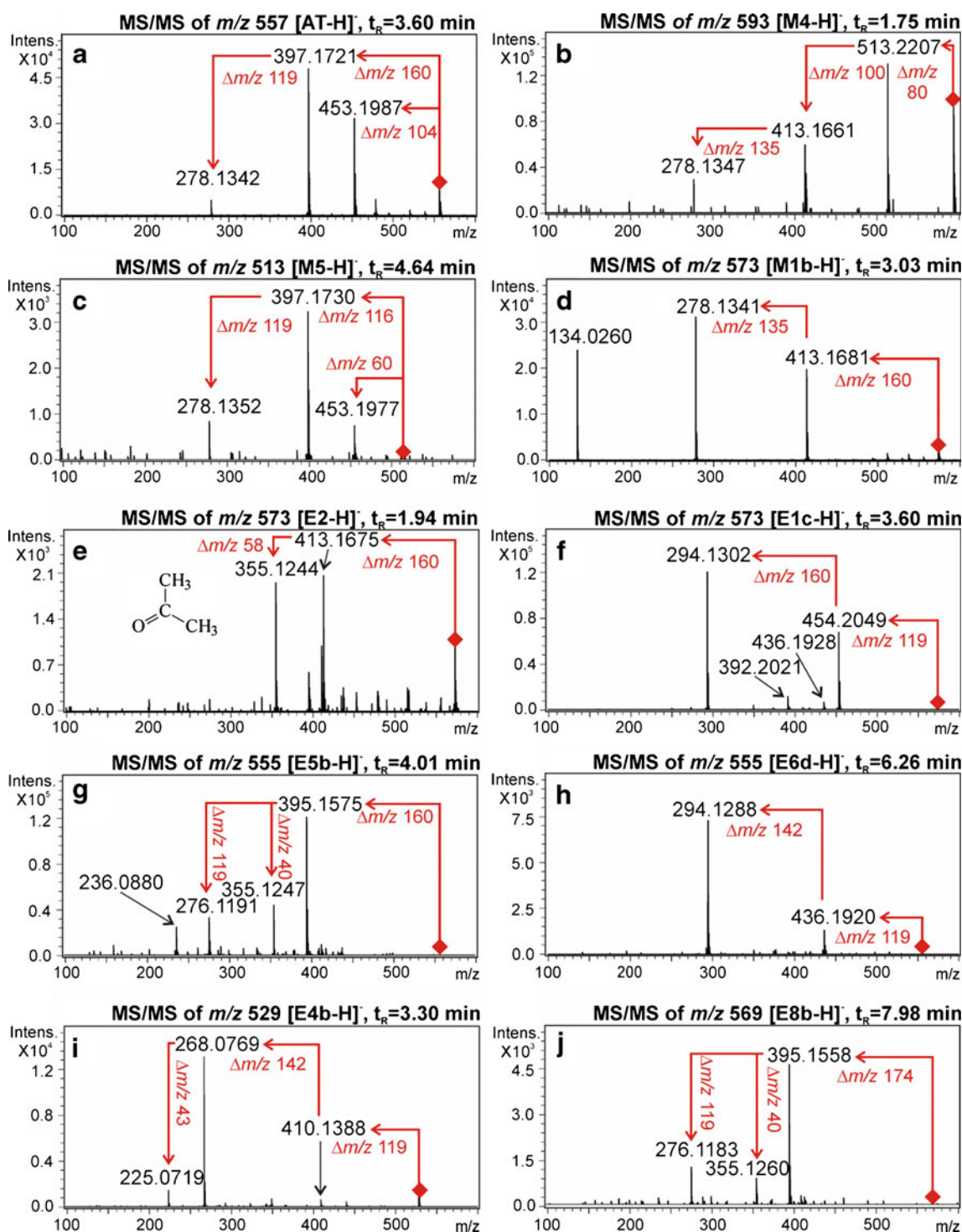


Fig. 8 ESI tandem mass spectra of deprotonated molecules of AT oxidation products (more information is given in Tables 1 and 2)

$\Delta m/z$ 144 in negative-ion mode and $\Delta m/z$ 132 in positive-ion mode were observed for glycol metabolites (M7 and M8). Information about all these structure modifications were often found by study of combined NLs, e.g., $\Delta m/z$ 235 (135+100, hydroxylation on AT part C and β -oxidation of AT part A), $\Delta m/z$ 261 (119+142, unchanged AT part C and lactone formation on AT part A), etc. Oxidation reactions on AT part B or

part D were observed for electrochemical samples. Observed NLs were mostly identical for the initial compounds (AT, ATL, or ATM), as evident from examples of tandem mass spectra in Fig. 8 and Table 2. The oxidation was mainly confirmed on the basis of key fragment ions m/z 308 (m/z 292 + O), 294 (m/z 278 + O), 290 (m/z 292 - H₂) and 276 (m/z 278 - H₂).

For better understanding of the correlation between modified structure and found NLs or fragment ions, a few examples of elucidation of the structures of selected oxidation products are given below. Tandem mass spectra shown in Fig. 8d, e, f illustrate the fragmentation of deprotonated molecules of oxidation products with identical molecular weights, 16 mass units higher than that of AT. Structure differences can be distinguished despite the identical chemical formula, $C_{33}H_{35}FN_2O_6$, of compounds E1a, b, c, E2, and M1a, b. AT part A is unchanged and the hydroxylation is ascribed to AT part C on the basis of NLs $\Delta m/z$ 135 and $\Delta m/z$ 160 in MS–MS of M1a (Fig. 8d) and M1b (not shown). Although some differences can be found between tandem mass spectra of the three isobaric compounds E1a, b, c, the exact position of oxidation cannot be determined by MS only. In general, all these oxidized products afford similar NLs, but in a different order of fragmentation. The ion at m/z 294 (Fig. 8f and Table 2) gives the most important information and confirms oxidation on part B. In contrast, no ion at m/z 294 is observed in MS–MS of E2 (Fig. 8e). The fragmentation of its deprotonated molecule with NL $\Delta m/z$ 160 yields the product ion at m/z 413. Subsequent NL of $\Delta m/z$ 58 results in the ion at m/z 355, which is indicative of oxidation of the isopropyl substituent. Another example is demonstrated by two groups of compounds E5 and E6 with the elemental composition $C_{33}H_{33}FN_2O_5$. The group of two compounds E5 belongs to dehydrogenated AT (AT – H₂, double bond formation or cyclization), whereas the second group including four E6 compounds is formed by addition of oxygen to ATL (ATL + O, hydroxylation or epoxidation). For E5, characteristic NLs $\Delta m/z$ 160 in negative-ion mode and $\Delta m/z$ 148 in positive-ion mode (Fig. 8g and Table 2) combined with NL $\Delta m/z$ 119 result in the formation of product ions at m/z 276 or 290 and are indicative of dehydrogenation of AT part B or D. Similarly, the NL $\Delta m/z$ 142 is present in negative-ion MS–MS of E6 or $\Delta m/z$ 130 in positive-ion MS–MS (Fig. 8h and Table 2) and in combination with NL $\Delta m/z$ 119 produce ions at m/z 294 and 308 (Table 2). Consequently, we can conclude that the initial compound was ATL and oxidation was by hydroxylation or epoxidation of AT part B. Unfortunately, fragment ions at m/z 276 and 294 have a stable conjugated system and they are not subsequently fragmented to furnish information about the exact position of oxidation. Determination of the exact position of oxidation for each group is not possible and requires additional analytical characterization. The last example is shown for double oxidized products E4. The nominal MW = 530 is possibly indicative of hydroxylated analogues of M3 (MW = 514), but the exact mass defect shows loss of propene and addition of two oxygen atoms compared with AT. Fragmentation of their deprotonated molecules is shown in Fig. 8i. The ion at m/z 410 is formed by NL $\Delta m/z$ 119 followed by the subsequent NL $\Delta m/z$ 142, resulting in the ion at m/z 268. Unlike above

mentioned examples of stable conjugated fragment ions at m/z 276 or 294, the product ion m/z 268 can be fragmented to provide the ion at m/z 225 formed after the NL $\Delta m/z$ 43 (NH=C=O) similarly to MS–MS of E4. On the basis of this information, oxidation is probably on the pyrrole ring.

Conclusions

In this work, electrochemically and *in-vitro*-generated AT oxidation products were studied in detail. Combined information from retention behavior in reversed-phase HPLC and mass spectrometry including high mass accuracy measurements in both full-scan and tandem mass spectra revealed 20 oxidation products in electrochemical samples and 10 metabolites after rat biotransformation. Although the structures of oxidative metabolites could not be precisely determined in some cases of isomeric compounds, tandem mass spectra provided enough information to decide which part of AT was modified. The rat *in-vitro* AT biotransformation resulted in β -oxidation, aromatic hydroxylation on the phenylaminocarbonyl group, sulfation of AT, and AT glycol formation, whereas electrochemical experiments resulted in a variety of oxidation reactions on the AT conjugated skeleton and the isopropyl substituent. Not surprisingly, AT is converted to ATL in acidic solution and oxidation reactions of ATL were observed together with AT oxidation products in electrochemical samples. The AT methyl ester and its oxidized products were also identified in electrochemical experiments. Comparison of fragmentation patterns with MS–MS of the initial compounds, i.e., AT, ATL, and ATM, has been successfully used to clarify the type of oxidative products. The importance of key NLs and fragment ions during structure elucidation is shown for several examples of differentiation of isobaric compounds. The approach reported herein can be further used in other studies of drug metabolism.

Acknowledgements This project was supported by the Czech Science Foundation (grant no. P206/12/P065). T.M. and V.Ch. acknowledge the support of Project No. CZ.1.07/2.3.00/30.0021 sponsored by the Ministry of Education, Youth and Sports of the Czech Republic.

References

1. Curran MP (2010) Amlodipine/Atorvastatin A Review of its Use in the Treatment of Hypertension and Dyslipidaemia and the Prevention of Cardiovascular Disease. *Drugs* 70:191–213
2. Bahrami G, Mohammadi B, Mirzaeei S, Kiani A (2005) Determination of atorvastatin in human serum by reversed-phase high-performance liquid chromatography with UV detection. *J Chromatogr B* 826:41–45
3. Nováková L, Satinský D, Solich P (2008) HPLC methods for the determination of simvastatin and atorvastatin. *Trends Anal Chem* 27:352–367

4. Farahani H, Norouzi P, Beheshti A, Sobhi HR, Dinarvand R, Ganjali MR (2009) Quantitation of atorvastatin in human plasma using directly suspended acceptor droplet in liquid–liquid–liquid microextraction and high-performance liquid chromatography–ultraviolet detection. *Talanta* 80:1001–1006
5. Shah Y, Iqbal Z, Ahmad L, Khan A, Khan MI, Nazir S, Nasir F (2011) Simultaneous determination of rosuvastatin and atorvastatin in human serum using RP–HPLC/UV detection: Method development, validation and optimization of various experimental parameters. *J Chromatogr B* 879:557–563
6. Bořek-Dohalský V, Huclová J, Barrett B, Němec B, Ulc I, Jelínek I (2006) Validated HPLC–MS–MS method for simultaneous determination of atorvastatin and 2-hydroxyatorvastatin in human plasma - pharmacokinetic study. *Anal Bioanal Chem* 386:275–285
7. Hermann M, Christensen H, Reubsaet JLE (2005) Determination of atorvastatin and metabolites in human plasma with solid-phase extraction followed by LC–tandem MS. *Anal Bioanal Chem* 382:1242–1249
8. Vlčková H, Solichová D, Bláha M, Solich P, Nováková L (2011) Microextraction by packed sorbent as sample preparation step for atorvastatin and its metabolites in biological samples–Critical evaluation. *J Pharm Biomed* 55:301–308
9. Macwan JS, Ionita IA, Dostalek M, Akhlaghi F (2011) Development and validation of a sensitive, simple, and rapid method for simultaneous quantitation of atorvastatin and its acid and lactone metabolites by liquid chromatography–tandem mass spectrometry (LC–MS–MS). *Anal Bioanal Chem* 400:423–433
10. Black AE, Sinz MW, Hayes RN, Woolf T (1998) Metabolism and excretion studies in mouse after single and multiple oral doses of the 3-hydroxy-3-methylglutaryl-CoA reductase inhibitor atorvastatin. *Drug Metab Dispos* 26:755–763
11. Nováková L, Vlčková H, Satinský D, Sadílek P, Solichová D, Bláha M, Bláha V, Solich P (2009) Ultra high performance liquid chromatography tandem mass spectrometric detection in clinical analysis of simvastatin and atorvastatin. *J Chromatogr B* 877:2093–2103
12. Prueksaritanont T, Subramanian R, Fang XJ, Ma B, Qiu Y, Lin JH, Pearson PG, Baillie TA (2002) Glucuronidation of statins in animals and humans: A novel mechanism of statin lactonization. *Drug Metab Dispos* 30:505–512
13. Jemal M, Zheng OY, Chen BC, Teitz D (1999) Quantitation of the acid and lactone forms of atorvastatin and its biotransformation products in human serum by high-performance liquid chromatography with electrospray tandem mass spectrometry. *Rapid Commun Mass Sp* 13:1003–1015
14. Kracun M, Kocijan A, Bastarda A, Grahek R, Plavec J, Kocjan D (2009) Isolation and structure determination of oxidative degradation products of atorvastatin. *J Pharm Biomed* 50:729–736
15. Shah RP, Kumar V, Singh S (2008) Liquid chromatography/mass spectrometric studies on atorvastatin and its stress degradation products. *Rapid Commun Mass Sp* 22:613–622
16. Jirásko R, Holčápek M, Vrublová E, Ulrichová J, Šimánek V (2010) Identification of new phase II metabolites of xanthohumol in rat in vivo biotransformation of hop extracts using high-performance liquid chromatography electrospray ionization tandem mass spectrometry. *J Chromatogr A* 1217:4100–4108
17. Jirásko R, Holčápek M, Nobilis M (2011) Identification of phase I and phase II metabolites of benfluron and dimefluron in rat urine using high-performance liquid chromatography/tandem mass spectrometry. *Rapid Commun Mass Sp* 25:2153–2162
18. Holčápek M, Kolářová L, Nobilis M (2008) High-performance liquid chromatography–tandem mass spectrometry in the identification and determination of phase I and phase II drug metabolites. *Anal Bioanal Chem* 391:59–78
19. Baumann A, Lohmann W, Schubert B, Oberacher H, Karst U (2009) Metabolic studies of tetrazepam based on electrochemical simulation in comparison to in vivo and in vitro methods. *J Chromatogr A* 1216:3192–3198
20. Faber H, Jahn S, Kunzemeyer J, Simon H, Melles D, Vogel M, Karst U (2011) Electrochemistry/Liquid Chromatography/Mass Spectrometry as a Tool in Metabolism Studies. *Angew Chem Int Edit* 50:A52–A58
21. Hoffmann T, Hofmann D, Klumpp E, Kuppers S (2011) Electrochemistry–mass spectrometry for mechanistic studies and simulation of oxidation processes in the environment. *Anal Bioanal Chem* 399:1859–1868
22. Johansson T, Weidolf L, Jurva U (2007) Mimicry of phase I drug metabolism - novel methods for metabolite characterization and synthesis. *Rapid Commun Mass Sp* 21:2323–2331
23. Karst U (2004) Electrochemistry/mass spectrometry (EG/MS) - A new tool to study drug metabolism and reaction mechanisms. *Angew Chem Int Edit* 43:2476–2478
24. Lohmann W, Karst U (2007) Generation and identification of reactive metabolites by electrochemistry and immobilized enzymes coupled on-line to liquid chromatography/mass spectrometry. *Anal Chem* 79:6831–6839
25. Lohmann W, Karst U (2008) Biomimetic modeling of oxidative drug metabolism. *Anal Bioanal Chem* 391:79–96
26. Lohmann W, Karst U (2009) Electrochemistry meets enzymes: instrumental on-line simulation of oxidative and conjugative metabolism reactions of toremifene. *Anal Bioanal Chem* 394:1341–1348
27. Nouri-Nigjeh E, Permentier HP, Bischoff R, Bruins AP (2011) Electrochemical Oxidation by Square-Wave Potential Pulses in the Imitation of Oxidative Drug Metabolism. *Anal Chem* 83:5519–5525
28. Odijk M, Baumann A, Olthuis W, van den Berg A, Karst U (2010) Electrochemistry-on-chip for on-line conversions in drug metabolism studies. *Biosens Bioelectron* 26:1521–1527
29. Baumann A, Karst U (2010) Online electrochemistry/mass spectrometry in drug metabolism studies: principles and applications. *Expert Opin Drug Met* 6:715–731
30. Lohmann W, Hayen H, Karst U (2008) Covalent Protein Modification by Reactive Drug Metabolites Using Online Electrochemistry/Liquid Chromatography/Mass Spectrometry. *Anal Chem* 80:9714–9719
31. Simon H, Melles D, Jacquilloet S, Sanderson P, Zazzeroni R, Karst U (2012) Combination of Electrochemistry and Nuclear Magnetic Resonance Spectroscopy for Metabolism Studies. *Anal Chem* 84:8777–8782
32. Nouri-Nigjeh E, Bischoff R, Bruins AP, Permentier HP (2011) Electrochemical oxidation by square-wave potential pulses in the imitation of phenacetin to acetaminophen biotransformation. *Analyst* 136:5064–5067
33. Jahn S, Lohmann W, Bomke S, Baumann A, Karst U (2012) A ferrocene-based reagent for the conjugation and quantification of reactive metabolites. *Anal Bioanal Chem* 402:461–471
34. van Leeuwen SM, Blankert B, Kauffmann JM, Karst U (2005) Prediction of clozapine metabolism by on-line electrochemistry/liquid chromatography/mass spectrometry. *Anal Bioanal Chem* 382:742–750
35. Jurva U, Wikstrom HV, Weidolf L, Bruins AP (2003) Comparison between electrochemistry/mass spectrometry and cytochrome P450 catalyzed oxidation reactions. *Rapid Commun Mass Sp* 17:800–810
36. Lohmann W, Baumann A, Karst U (2010) Electrochemistry and LC–MS for Metabolite Generation and Identification: Tools, Technologies, and Trends. *Lc Gc N Am* 28:470–■
37. Holčápek M, Jirásko R, Lisa M (2012) Recent developments in liquid chromatography–mass spectrometry and related techniques. *J Chromatogr A* 1259:3–15
38. Holčápek M, Jirásko R, Lisa M (2010) Basic rules for the interpretation of atmospheric pressure ionization mass spectra of small molecules. *J Chromatogr A* 1217:3908–3921
39. Staack RF, Hopfgartner G (2007) New analytical strategies in studying drug metabolism. *Anal Bioanal Chem* 388:1365–1380
40. Laphorn C, Pullen F, Chowdhry BZ (2013) Ion mobility spectrometry–mass spectrometry (IMS–MS) of small molecules: Separating and assigning structures to ions. *Mass Spectrom Rev* 32:43–71

41. Liu DQ, Hop C (2005) Strategies for characterization of drug metabolites using liquid chromatography–tandem mass spectrometry in conjunction with chemical derivatization and on-line H/D exchange approaches. *J Pharm Biomed* 37:1–18
42. Meyer MR, Maurer HH (2012) Current applications of high-resolution mass spectrometry in drug metabolism studies. *Anal Bioanal Chem* 403:1221–1231
43. Prakash C, Shaffer CL, Nedderman A (2007) Analytical strategies for identifying drug metabolites. *Mass Spectrom Rev* 26:340–369
44. Prasad B, Garg A, Takwani H, Singh S (2011) Metabolite identification by liquid chromatography–mass spectrometry. *Trends Anal Chem* 30:360–387
45. Zhu MS, Zhang HY, Humphreys WG (2011) Drug Metabolite Profiling and Identification by High-resolution Mass Spectrometry. *J Biol Chem* 286:25419–25425
46. Ghosh C, Jain I, Gaur S, Patel N, Upadhyay A, Chakraborty BS (2011) Simultaneous estimation of atorvastatin and its two metabolites from human plasma by ESI–LC–MS–MS. *Drug Test Anal* 3:352–362
47. Mikysek T, Švancara I, Bartoš M, Vytřas K, Drabina P, Sedlák M, Klíma J, Urban J, Ludvík J (2007) Electrochemical studies on new chelating compounds of the mono- and bis(imidazolyl)pyridine type. *Electroanal* 19:2529–2537



Robert Jirásko is a researcher with the mass spectrometry group at the Department of Analytical Chemistry, University of Pardubice, Czech Republic. His research interests are the development of methods in separation techniques, mass spectrometry, and MS imaging, and the application of these in studies of drug metabolism



Tomáš Mikysek is a senior researcher at the Department of Analytical Chemistry, University of Pardubice, Czech Republic. He is working on molecular electrochemistry with a focus on the electrochemical characterization of organic compounds and studies on the reaction mechanism of electrode reactions



Vitaliy V. Chagovets is a researcher with the Department of Analytical Chemistry, University of Pardubice, Czech Republic. His research interests are the development of desorption techniques in mass spectrometry, mass spectrometric instrumentation and software, and the use of these to solve problems in analytical chemistry, molecular biology, and nanotechnology



Ivan Vokřál is an Assistant Professor at the Department of Pharmacology and Toxicology, Faculty of Pharmacy in Hradec Králové, Charles University in Prague, Czech Republic. His fields of interest are liquid chromatography–mass spectrometry, parasitology, and molecular biology, mostly in connection with drug resistance and drug metabolism by parasites



Michal Holčapek is currently working as a full-time professor and is head of the mass spectrometry group at the Department of Analytical Chemistry, University of Pardubice, Czech Republic. He also acts as national representative for the Czech Republic at the International Mass Spectrometry Foundation. His research interests are mass spectrometry and its coupling with liquid-phase separation techniques, with specialization in analysis of the structures of (bio)organic and organometallic compounds, mainly lipidomics, metabolomics, and drug metabolites